Biosensors and Bioelectronics 129 (2019) 87–92

Contents lists available at ScienceDirect

Biosensors and Bioelectronics

journal homepage: www.elsevier.com/locate/bios

Optical fiber amplifier for quantitative and sensitive point-of-care testing of myoglobin and miRNA-141

Xiaofeng Liu[1], Hua Zhang[1], Shiya Qin, Qing Wang*, Xiaohai Yang, Kemin Wang*

State Key Laboratory of Chemo/Biosensing and Chemometrics, College of Chemistry and Chemical Engineering, Key Laboratory for Bio-Nanotechnology and Molecular Engineering of Hunan Province, Hunan University, Changsha 410082, China

ARTICLE INFO

Keywords:
Optical fiber amplifier
Point-of-care testing
Myoglobin
MiRNA-141

ABSTRACT

A simple, sensitive, quantitative point-of-care testing (POCT) was developed integrating enzyme-linked DNA supersandwich amplification with optical fiber amplifier. The point-of-care (POC) assay can work in both "Turn-off" mode and "Turn-on" mode. Using myoglobin (Myo) and miRNA-141 as the model biomarker, as low as 0.5 nM Myo and 10 pM miRNA-141 could be detected. More importantly, the optical fiber amplifier, which was used as signal readout, exhibited low-cost, small size, rapid response, and easy operation. Although it did not need large equipment and professional technical personnel, the assay was successfully applied to detect Myo and miRNA-141 in 40% human serum. Since the entire process of the strategy could be done directly in the centrifugal tube, requiring a few easy steps, it showed great potential application for early diagnosis in the world, especially in developing countries or remote regions. This work provided a new avenue for developing the portable and sensitive biosensor.

1. Introduction

Point-of-care testing (POCT) offered the advantages of simple, sensitive, rapid, portable, equipment-free, user-friendly, and inexpensive measurement (Bandodkar et al., 2016; Clerc and Greub, 2010; Cui et al., 2017; Song et al., 2017). The development and popularization of POCT was of vital importance in healthcare diagnostics, food safety assessment, and environmental monitoring, especially in the situations lacking laboratory equipment (Chen et al., 2017; Giljohann and Mirkin, 2009; Gubala et al., 2012; Xiang and Lu, 2011). In recent years, considerable effort has been devoted to the development of POCT devices, such as patterned paper devices (Tenda et al., 2018), visual detection sensors (Ayaz Ahmed et al., 2016; Hou et al., 2018; Jung and Park, 2015), microfluidic systems (Li et al., 2016; Xie et al., 2016) and other novel platform (Shi et al., 2018; Zhang et al., 2018; Zhu et al., 2015).

Since color changes could be easily observed using naked eye, colorimetric assay has attracted increasing attention for in situ analysis and point of-care diagnosis such as lateral-flow colorimetric assay, nanoparticles aggregation-based colorimetric assay and enzyme-mediated colorimetric assay (Calabria et al., 2017; Huang et al., 2013; Jung and Park, 2015; Song et al., 2011; Tian et al., 2016). Generally, most of traditional colorimetric based point-of-care platforms provided only qualitative and not quantitative data (Guler et al., 2017; Ouyang et al., 2018; Qi et al., 2018). Therefore, it is of great value to develop a rapid, low-cost, and sensitive colorimetric assay based POCT which can achieve quantitative analysis.

Recently, fiber optic sensors developed rapidly in chemical, environmental, and biochemical area due to the rise of fiber optics technology (Fong et al., 2015; Wolfbeis, 2004). However, it was hard for traditional fiber optic device with professional staff and high cost to achieve POC testing. Optical fiber amplifier (OFA), which uses LED as light source and photodiode as detector, generally monitors the change of light intensity. Due to its low-cost, small size, rapid response, easy operation, high credibility, free switching in a variety of modes and avoiding the interference from outside light, OFA may become promising candidates for POCT diagnostic platforms.

Here, a simple, easy-to-use POC assay with high sensitivity and convenient readout was introduced. In this POC assay, DNA supersandwich was used for signal amplification and OFA was used for signal readout. Protein and nucleic acid are very important component of cells and tissues and their levels are associated with diseases (Li et al., 2012; Luan et al., 2018; Pan et al., 2018; Yang et al., 2016; Zhao et al., 2018). Myoglobin (Myo), the early biomarker for acute myocardial infarction (AMI) (Matveeva et al., 2004; Moreira et al., 2011; Wang et al., 2015a, 2015b, 2015c), and miRNA-141 (Wang et al., 2016), the biomarker of prostate cancer, were chosen as model target. "Turn-off" mode and

* Corresponding authors.
E-mail addresses: wwqq99@hnu.edu.cn (Q. Wang), kmwang@hnu.edu.cn (K. Wang).
[1] Contributed equally.

https://doi.org/10.1016/j.bios.2018.12.056
Received 18 November 2018; Received in revised form 15 December 2018; Accepted 18 December 2018
Available online 18 January 2019
0956-5663/

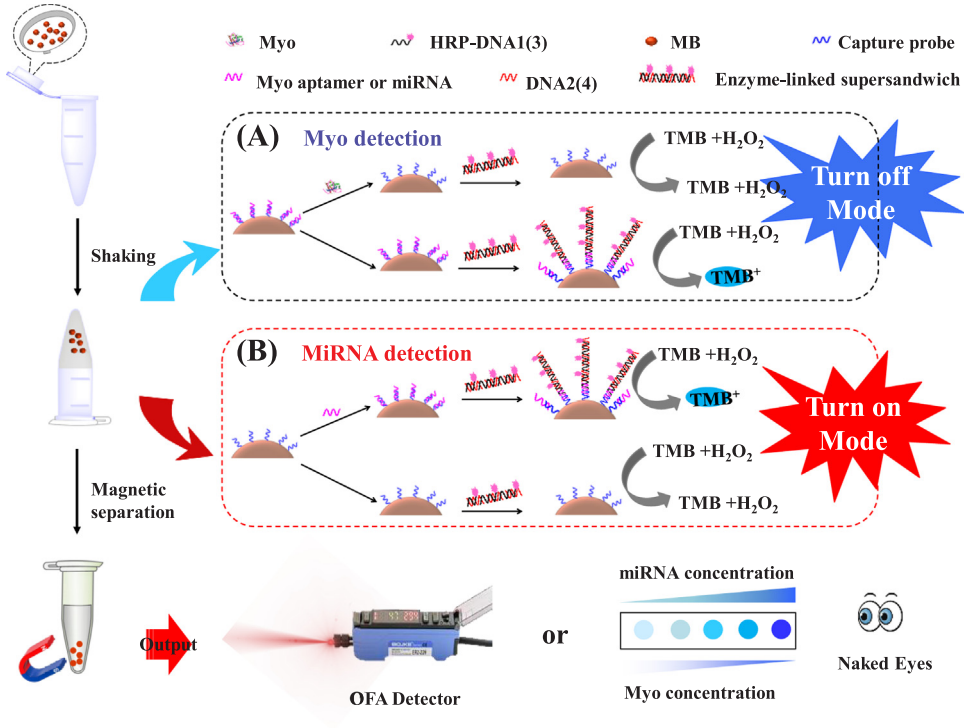

Fig. 1. The schematic illustration of the portable OFA aptsensor for the sensitive detection of Myo and miRNA-141.

"Turn-on" mode were designed for quantitative POCT of Myo and miRNA-141, respectively. The principle of this assay for Myo detection was shown in Fig. 1A. Firstly, biotin-labelled capture probe was immobilized onto the streptavidin-linked magnetic bead (MB). After the aptamer against Myo, which was screened by our lab (Wang et al., 2014a), was added, the aptamer could bind on the MB through the hybridization with capture probe. Subsequently, in the absence of target Myo, the aptamer on the MB could hybridize with enzyme-linked supersandwich products which were synthetized by the hybridization of horseradish peroxidase (HRP)-DNA1 and DNA2, resulting in a plurality of HRP on the MB. Then the HRP transduced the sensing events through the catalyzed H_2O_2-mediated oxidation of TMB from colorless to blue in solution with an absorption maximum at $\lambda = 651$ nm. While in the presence of Myo, the interaction between aptamer and Myo displaced the aptamer from the MB, resulting in the decrease of the amount of enzyme-linked DNA supersandwich products on the MB. Consequently, almost no color change occurred after the addition of TMB and H_2O_2. The final color changes were directly proportional to the concentration of Myo and easily visually distinguished by naked eye (qualitative detection) and OFA (quantitative detection), respectively. Fig. 1-B showed the principle of POC assay for miRNA-141 detection. Biotin-labelled capture probe was first immobilized onto streptavidin-linked MB. In the presence of target miRNA-141, it was complementary to capture probe A on the MB at the one-half-segment and complementary to enzyme-linked supersandwich products, which were formed through the hybridization of HRP-DNA3 and DNA4, at the other half-segment. It resulted in a plurality of HRP on the MB. Subsequently, the HRP efficiently catalyzed the oxidation of TMB, resulting in the appearance of blue color solution. On the contrary, in the absence of miRNA-141, capture probe on MB could not hybridize with enzyme-linked supersandwich product. Consequently, almost no color change occurred after the addition of TMB and H_2O_2. According to the change of solution, the concentration of miRNA-141 could also be detected by OFA or naked eye. The entire process of the method can be done directly in the centrifugal tube, requiring a few easy steps. Moreover, the POC assay exhibited excellent practical applications for Myo and miRNA-141 detection in serums, which presented potential applications in biological detection and clinical diagnosis. Theoretically, it could potentially be used for POC detection of other targets, as long as an appropriate probe can be found and replaced.

2. Experimental

2.1. Reagents

Myo protein (from human heart tissue) was purchased from Abcam (USA). Horseradish peroxidase (HRP), alkaline phosphatase (ALP), glucose oxidase (Gox), tris (2-carboxyethyl) phosphine hydrochloride (TCEP), sulfosuccinimidyl-4-(N-maleimidomethyl) cyclohexane-1-carboxylate (sulfo-SMCC) and 3, 3′, 5, 5′-tetramethylbenzidine (TMB) were obtained from Sigma-Aldrich (St. Louis, MO, U.S.A.). C reactive protein (CRP) was purchased from Biovision (USA). Bovine serum albumin (BSA) and human serum albumin (HSA) were purchased from Beijing Dingguo Changsheng Biotechnology Co., Ltd. (China). Dynabeads M-280 streptavidin magnetic bead (MB) was purchased from Invitrogen (AS, Oslo, Norway). All the chemical reagents were of analytical grade and used without further purification. Ultrapure water (18.2 MΩ·cm) was used throughout. DNA probes, which were listed in Table S-1 and diethylpyrocarbonatex (DEPC) were purchased from Sangon Biotech. Co., Ltd. (Shanghai, China). The solutions for miRNA detection were treated with DEPC and autoclaved to protect from RNase degradation. Serum samples were collected from healthy volunteers.

2.2. Operating procedures of optical fiber amplifier (OFA)

OFA, which uses LED as light source and photodiode as detector, generally monitors the change of light intensity. The photograph was shown in Fig. S-1. It generally includes mode from *P*-1 to P-8. The mode means the sensitivity of the OFA device. The higher the number of the mode, the lower the sensitivity. Here P-2 was selected in POC assay for target detection. For target detection, the reaction solution without target was first measured using OFA and the value was recorded as I_0. Then different concentrations of target were added. After reacted with functionalized magnetic bead, the enzyme-linked supersandwich

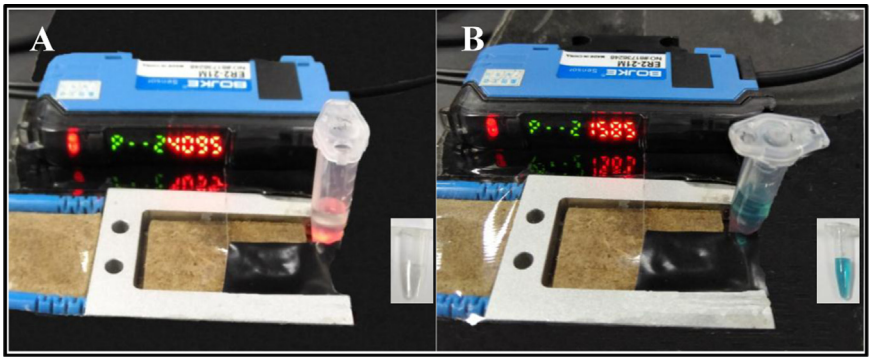

Fig. 2. Photograph of OFA signal in the presence of Myo (A) and in the absence of Myo (B).

products was added. After magnetic separation, the supernatant was discarded. Next, TMB and H_2O_2 were added. After magnetic separation, the supernatant was directly measured using OFA and the value was recorder as I. The light intensity change ratio $I\text{-}I_0$ was represented as a signal analysis parameter.

2.3. Preparation and characterization of HRP-DNA conjugate

The synthesis of HRP-DNA conjugate was similar to the previous work (Wang et al., 2014a, 2014b). Take HRP-DNA1 for an example, the DNA1 was first modified with sulfhydryl at the 5′ end. Then sulfo-SMCC was used as a linker to conjugate DNA1 and HRP. HRP-DNA1 conjugate was characterized using a 12% SDS-PAGE experiment.

2.4. Preparation and characterization of enzyme-linked supersandwich products

Enzyme-linked supersandwich products was prepared as follows: The DNA1-HRP and DNA2 were incubated at 37 °C for 1 h. Preparation of the supersandwich structures was investigated using agarose gel electrophoresis. In the gel electrophoresis assay, 2 μL 6 × loading buffer, 2 μL of SYBR Gold and 10 μL of reaction sample was subjected to the 2% agarose gel electrophoresis. The gel was prepared using a 1 × TBE buffer and were run at 90 V for 40 min.

2.5. Preparation of capture probe-aptamer modified MB

The capture probe-aptamer modified MB was prepared as follows: The biotinylated capture probe (200 nM) and Myo aptamer (200 nM) were incubated with the streptavidin MB at 25 °C for 60 min. Next, the MB was collected by magnetic separator, and then resuspended with 20 mM HEPES buffer (pH 7.35). The capture probe-aptamer modified MB was stored at 4 °C for further use.

3. Results and discussion

3.1. Characterization of HRP-DNA conjugate and enzyme-linked supersandwich products

Due to the importance of the enzyme-linked supersandwich products, the agarose gel electrophoresis assay was first used for investigating the formation of the enzyme-linked supersandwich products. As shown in Fig. S-2, the band of HRP in the lane 1 was located under 44.3 kDa, which was in agreement with the molecular weight of HRP (ca. 44 kDa). Upon conjugation with DNA1, the migration of the HRP-DNA1 conjugate band in the lane 2 was less than that of HRP. Presumably, DNA1 conjugated with HRP, resulting in the increase of the molecular weight. In addition, since DNA1 was not conjugated with HRP in the mixture of DNA1 and HRP, little difference was observed between lane 1 and lane 3. The results demonstrated that the HRP-DNA1 conjugate was formed. In addition, as shown in Fig. S-3, the mixture of DNA1 and DNA2 could hybridize with each other and form longer DNA fragments (lane 4), suggesting the formation of supersandwich. At the same time, the mixture of HRP-DNA1 and DNA2 also produced a ladder of different lengths of the supersandwich structure (lane 5). The results confirmed the formation of the multiplex HRP-DNA supersandwich nanostructures. As shown in Fig. S-2 and S-3, the results demonstrated that the enzyme-linked supersandwich products were easily formed.

3.2. Investigation of loading efficiency on the MB

The loading efficiency on the MB was characterized using UV–vis analysis. The details were shown as follows: different concentrations of biotinylated capture probe (C_1) were incubated with 2 mg/mL MB solution at 25°C for 60 min. Next, the MB was removed by magnetic separator and the supernatant was measured using UV–Vis spectrometer. The concentration of capture probe in the supernatant (C_2) was estimated according to the absorption at 260 nm. Then the concentration of capture probe modified on the MB (C_3) was calculated according to the equation $C_3 = C_1\text{-}C_2$. As shown in Fig. S-4, C_3 increased with the increase of C_1 until the C_1 was 100 pM. The result demonstrated that ca. 212.5 pM biotinylated capture probe were modified on 1 mg MB.

3.3. The feasibility of proposed method by OFA

As shown in Fig. 2, the OFA was used with the U-shaped fiber. Take the Myo detection as an example, given that few or no blue products (TMB^+) were obtained in the presence of 500 nM Myo, the intensity of light from LED was almost not influenced, resulting in large OFA signal (shown in Fig. 2A). On the contrary, lots of blue products were produced as the target Myo was absent and the light intensity was significantly reduced consequently, resulting in the decrease of OFA signal (shown in Fig. 2B). Thus, the concentration of target Myo would be estimated according to the change of light intensity. Here, light intensity change ($I\text{-}I_0$) was represented as a signal analysis parameter, where I and I_0 were the light intensity detected using OFA in the presence or absence of target Myo, respectively. Furthermore, take the Myo detection as an instance, the feasibility of this assay was also investigated using UV–vis spectroscopy. As shown in Fig. S-5, it presented the strong absorption peak at $\lambda = 651$ nm in the absence of Myo. While weak absorption peak at $\lambda = 651$ nm was showed in the presence of Myo. The result also implied that the proposed method had the excellent feasibility.

3.4. Myo detection using POC assay

Given that different experimental parameters, such as the sequence of capture probe, the temperature, the incubation time of Myo and aptamer on the MB, the incubation time of supersandwich products and

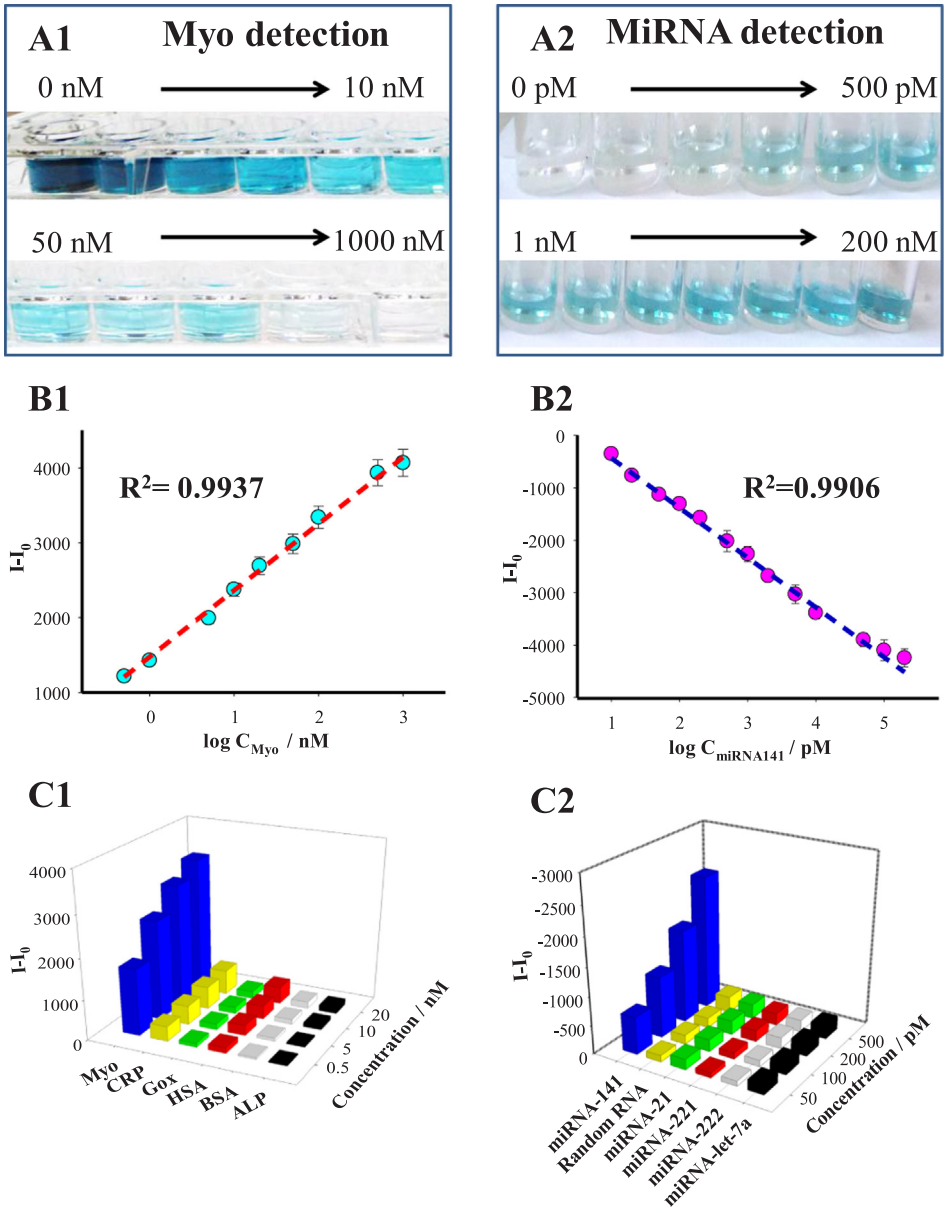

Fig. 3. (A) The photograph of detecting different concentrations of Myo (A1) and miRNA-141 (A2). (B)The relationship between ($I-I_0$) and concentrations of Myo (B1) and miRNA-141 (B2) using the POC assay. (C) Selectivity investigation of the POC assay for detection of Myo (C1) and miRNA-141(C2), respectively.

aptamer on the MB, and the concentration of H_2O_2, could influence the performance of the detection system, the effects of these factors were investigated using UV–vis spectroscopy. As shown in Fig. S-6, capture probe 2, 25 °C of reaction temperature, 75 min incubation time with Myo, 90 min incubation time with supersandwich products, 0.15 mM H_2O_2 concentration were chosen in the following experiment. Furthermore, as shown in Fig. S-7, comparing with HRP amplified detection, the signal was obvious enhanced using enzyme-linked supersandwich amplified detection, demonstrating that the amplification efficiency of enzyme-linked supersandwich strategy was excellent.

Under the optimal experimental conditions, the sensitivity of the POC detection of Myo was investigated using naked eyes and the OFA, respectively. Fig. 3A1 showed the concentration profile for the Myo-induced color change. The solution gradually became lighter with an increase of Myo concentration, suggesting a decrease of the enzyme-linked supersandwich products on the magnetic bead. As the OFA was used as a signal readout, it was shown in Fig. 3B1 that ($I-I_0$) increased with the increase of Myo concentration from 0 to 400 nM. The linear regression curve was $I-I_0 = 981.3 \log [Myo] + 1384.6$ with a good linearity ($R^2 = 0.9937$) (Fig. 3B1). As low as 0.5 nM Myo could be detected. It was lower than the clinical cutoff Myo concentration (5.4 nM) (Matveeva et al., 2004), implying that the assay could be used in clinical diagnosis of AMI. The result also showed good accordance with that of UV–Vis spectrophotometer (S-3). Besides, the sensitive was comparable to or better than that of the previous works (Moreira et al., 2011; Song et al., 2017; Wang et al., 2015c).

To evaluate the selectivity of the proposed POC assay for Myo detection, the effects of five kinds of protein, including C reactive protein (CRP), glucose oxidase (Gox), human serum albumin (HSA), bovine serum albumin (BSA) and alkaline phosphatase (ALP) were investigated. The system only showed a remarkable light intensity in the presence of Myo. Nevertheless, the light intensity was negligible in the presence of CRP, Gox, HSA, BSA and ALP, respectively (Fig. 3C1). The result was consistent with that using UV–Vis spectrophotometer (Fig. S-8), demonstrating that the proposed POC assay had excellent selectivity for target Myo.

To investigate the capacity of the proposed POC assay for Myo detection in real sample, human serum as model matrix were employed.

Table 1
Detection of Myo in human serum sample based on proposed POC assay.

Sample	Added Myo (nM)	Detected Myo (nM)	Recovery (%)	RSD (n = 3, %)
1	5	5.2	105.0	1.2
	20	20.4	102.1	2.8
	100	99.6	99.6	2.4
	500	499.5	99.9	5.1
2	5	4.9	98.0	3.2
	20	20.1	101.0	4.1
	100	98.3	98.3	4.6
	500	501.6	101.0	5.9

Table 2
Detection of miRNA-141 in human serum sample based on proposed POC assay.

Sample	Added miRNA-141 (pM)	Detected miRNA-141 (pM)	Recovery (%)	RSD (n = 3, %)
1	50	52.2	104.4	3.4
	100	97.7	97.7	2.9
	200	201.3	100.7	3.1
	500	497.9	99.6	4.3
2	50	49.6	99.2	2.7
	100	101.9	101.9	4.1
	200	197.2	98.6	5.3
	500	503.1	100.6	3.1

In brief, a series of concentrations of Myo (40 μL) were first spiked into 60 μL untreated serum samples, and the final concentration of the serum was 40%. Next, the Myo-spiked serum samples were directly detected without other operation. As shown in Table 1, the recoveries varied from 98.0% to 105.0%, and the relative standard deviation (RSD) was from 1.2% to 5.9%. The result also showed good accordance with that of UV–Vis spectrophotometer (Table S2). It illustrated that OFA may be a promising way for Myo detection in clinical diagnosis.

3.5. MiRNA-141 detection using POC assay

Besides, miRNA-141 was also detected using the POC assay. As shown in Fig. 3A2, the solution color gradually changed from blank to blue with the increase of miRNA-141 concentration. The signal ($I-I_0$) gradually decreased as the increase of miRNA-141 in the range from 0.0 to 200.0 nM, as shown in Fig. 3B2. In addition, the regression equation was $I-I_0 = -984.7 \log[\text{miRNA}] + 514.2$ with a correlation coefficient R^2 of 0.9906 and the detection limit was estimated in term of this fitting curve was 10 pM (S/N = 3), which was comparable to or better than that of the previous works (Shi et al., 2018; Xiang and Lu, 2012a, 2012b). To evaluate the specificity of the proposed POC assay, miRNA-141, miRNA-221, miRNA-let7a, miRNA-21 and random miRNA were used for analysis. The system only showed a remarkable light intensity in the presence of miRNA-141. Nevertheless, the light intensity was negligible in the presence of miRNA-221, miRNA-let7a, miRNA-21 and random miRNA (as shown in Fig. 3C2). The results showed that had excellent selectivity for miRNA-141 against other miRNAs. In addition, the proposed POC assay was also employed to detect miRNA-141 in human serum samples. The human normal serum (regarding that not contain miRNA in detectable quantity) was first treated with the RNase inhibitor to remove miRNA. The other steps were the same with Myo detection in human serum samples. The results were shown in Table 2. The recoveries varied from 98.6% to 104.4%, and the relative standard deviation (RSD) was from 2.7% to 5.3%. The results indicated that the proposed POC assay has potential applications for miRNA in real samples.

4. Conclusions

In conclusion, a simple, disposable, sensitive qualitative and quantitative POCT platform based on OFA was developed for the detection of Myo and miRNA-141. It was the first time that OFA was used as signal readout for POCT. This method did not need large equipment and professional technical personnel. The POC assay could detect as low as 0.5 nM Myo and 10 pM miRNA-141 (3σ). In addition, since the entire process of the strategy could be done directly in the centrifugal tube, requiring a few easy steps, it showed great potential application for early diagnosis in the world, especially in developing countries or remote regions. Theoretically, this assay could potentially develop novel POCT for detection of other targets, if an appropriate probe can be found and replaced. This work opens up a new way for simple, portable, and sensitive biosensing.

CRediT authorship contribution statement

Xiaofeng Liu: Data curation, Validation, Visualization, Writing - original draft. **Hua Zhang:** Data curation, Validation, Visualization. **Shiya Qin:** Investigation. **Qing Wang:** Funding acquisition, Project administration, Supervision, Writing - review & editing. **Xiaohai Yang:** Conceptualization, Methodology, Supervision. **Kemin Wang:** Funding acquisition, Project administration.

Acknowledgments

This work was supported by the National Natural Science Foundation of China (21675047, 21375034 and 21735002), and National Science Foundation for Distinguished Young Scholars of Hunan Province (2016JJ1008).

Appendix A. Supplementary material

Supplementary data associated with this article can be found in the online version at doi:10.1016/j.bios.2018.12.056.

References

Ayaz Ahmed, K.B., Sengan, M., P, S.K., Veerappan, A., 2016. Sens. Actuators B: Chem. 233, 431–437.
Bandodkar, A.J., Jeerapan, I., Wang, J., 2016. ACS Sens. 1 (5), 464–482.
Calabria, D., Caliceti, C., Zangheri, M., Mirasoli, M., Simoni, P., Roda, A., 2017. Biosens. Bioelectron. 94, 124–130.
Chen, Y., Xianyu, Y., Wu, J., Dong, M., Zheng, W., Sun, J., Jiang, X., 2017. Anal. Chem. 89 (10), 5422–5427.
Clerc, O., Greub, G., 2010. Clin. Microbiol. Infect. 16 (8), 1054–1061.
Cui, X., Das, A., Dhawane, A.N., Sweeney, J., Zhang, X., Chivukula, V., Iyer, S.S., 2017. Chem. Sci. 8 (5), 3628–3634.
Fong, J.K., Pena, J.K., Xue, Z.L., Alam, M.M., Sampathkumaran, U., Goswami, K., 2015. Anal. Chem. 87 (3), 1569–1574.
Giljohann, D.A., Mirkin, C.A., 2009. Nature 462 (7272), 461–464.
Gubala, V., Harris, L.F., Ricco, A.J., Tan, M.X., Williams, D.E., 2012. Anal. Chem. 84 (2), 487–515.
Guler, E., Yilmaz Sengel, T., Gumus, Z.P., Arslan, M., Coskunol, H., Timur, S., Yagci, Y., 2017. Anal. Chem. 89 (18), 9629–9632.
Hou, Y., Wang, J., Jiang, W., Lv, C., Xia, L., Hong, S., Lin, M., Lin, Y., Zhang, Z., Pang, D.W., 2018. Biosens. Bioelectron. 99, 186–192.
Huang, H., Jin, L., Yang, X., Song, Q.X., Zou, B.J., Jiang, S.W., Sun, L.Z., Zhou, G.H., 2013. Biosens. Bioelectron. 42, 261–266.
Jung, Y.K., Park, H.G., 2015. Biosens. Bioelectron. 72, 127–132.
Li, N., Chang, C., Pan, W., Tang, B., 2012. Angew. Chem. Int. Ed. 51 (30), 7426–7430.
Li, Y., Xuan, J., Song, Y., Qi, W., He, B., Wang, P., Qin, L., 2016. ACS Nano 10 (1), 1640–1647.
Luan, M., Chang, J., Pan, W., Chen, Y., Li, N., Tang, B., 2018. Anal. Chem. 90 (18), 10951–10957.
Matveeva, E., Gryczynski, Z., Gryczynski, I., Malicka, J., Lakowicz, J.R., 2004. Anal. Chem. 76 (21), 6287–6292.
Moreira, F.T., Dutra, R.A., Noronha, J.P., Sales, M.G., 2011. Biosens. Bioelectron. 26 (12), 4760–4766.
Ouyang, H., Lu, Q., Wang, W., Song, Y., Tu, X., Zhu, C., Smith, J.N., Du, D., Fu, Z., Lin, Y., 2018. Anal. Chem. 90 (8), 5147–5152.
Pan, W., Liu, B., Gao, X., Yu, Z., Liu, X., Li, N., Tang, B., 2018. Nanoscale 10 (29), 14264–14271.

Qi, L., Hu, Q., Kang, Q., Yu, L., 2018. Anal. Chem. 90 (19), 11607–11613.
Shi, L., Lei, J., Zhang, B., Li, B., Yang, C.J., Jin, Y., 2018. ACS Appl. Mater. Interfaces 10 (15), 12526–12533.
Song, Y., An, Y., Liu, W., Hou, W., Li, X., Lin, B., Zhu, Z., Ge, S., Yang, H.H., Yang, C., 2017. Chem. Commun. 53 (86), 11774–11777.
Song, Y., Wei, W., Qu, X., 2011. Adv. Mater. 23 (37), 4215–4236.
Tenda, K., van Gerven, B., Arts, R., Hiruta, Y., Merkx, M., Citterio, D., 2018. Angew. Chem. Int. Ed. 57 (47), 15369–15373.
Tian, T., Wei, X.F., Jia, S.S., Zhang, R.H., Li, J.X., Zhu, Z., Zhang, H.M., Ma, Y.L., Lin, Z.Y., Yang, C.J., 2016. Biosens. Bioelectron. 77, 537–542.
Wang, Q., Li, Q., Yang, X., Wang, K., Du, S., Zhang, H., Nie, Y., 2016. Biosens. Bioelectron. 77, 1001–1007.
Wang, Q., Liu, F., Yang, X., Wang, K., Wang, H., Deng, X., 2015a. Biosens. Bioelectron. 64, 161–164.
Wang, Q., Liu, L., Yang, X., Wang, K., Chen, N., Zhou, C., Luo, B., Du, S., 2015b. Anal. Chem. 87 (4), 2242–2248.
Wang, Q., Liu, W., Xing, Y., Yang, X., Wang, K., Jiang, R., Wang, P., Zhao, Q., 2014a. Anal. Chem. 86 (13), 6572–6579.
Wang, Q., Wang, H., Yang, X., Wang, K., Liu, F., Zhao, Q., Liu, P., Liu, R., 2014b. Chem. Commun. 50 (29), 3824–3826.
Wang, Q., Yang, X., Yang, X., Liu, F., Wang, K., 2015c. Sens. Actuators B: Chem. 212, 440–445.
Wolfbeis, O.S., 2004. Fiber-optic chemical sensors and biosensors. Anal. Chem. Anal. Chem. 76 (12), 3269–3283.
Xiang, Y., Lu, Y., 2011. Nat. Chem. 3 (9), 697–703.
Xiang, Y., Lu, Y., 2012a. Anal. Chem. 84 (9), 4174–4178.
Xiang, Y., Lu, Y., 2012b. Anal. Chem. 84 (4), 1975–1980.
Xie, Y., Wei, X., Yang, Q., Guan, Z., Liu, D., Liu, X., Zhou, L., Zhu, Z., Lin, Z., Yang, C., 2016. Chem. Commun. 52 (91), 13377–13380.
Yang, L., Ren, Y., Pan, W., Yu, Z., Tong, L., Li, N., Tang, B., 2016. Anal. Chem. 88 (23), 11886–11891.
Zhang, J., Xing, H., Lu, Y., 2018. Chem. Sci. 9 (16), 3906–3910.
Zhao, M.S., Zhang, S.S., Chen, Z.Q., Zhao, C.Z., Wang, L., Liu, S.F., 2018. Biosens. Bioelectron. 105, 42–48.
Zhu, Z., Guan, Z.C., Liu, D., Jia, S.S., Li, J.X., Lei, Z.C., Lin, S.C., Ji, T.H., Tian, Z.Q., Yang, C.Y.J., 2015. Angew. Chem. Int. Ed. 54 (36), 10448–10453.